[PROC. OF JSCE No. 396/V-9 (Concrete Eng. and Pavements) August 1988]

A STUDY ON FATIGUE BEHAVIOR OF COLD-WORKED DEFORMED REINFORCING BARS

*By Nobuyuki MATSUMOTO**

This test program was implemented to determine the fatigue behavior of reinforcing bars in air and the effect of cold-work on fatigue strength. A lot of studies have been conducted to investigate the fatigue behavior of reinforcing bars embedded in concrete beam, however, only few studies have been reported for reinforcing bars alone. This test was performed to provide information that may aid in interpretation of beam fatigue test. Fatigue characteristics of cold-worked (pre-strained) reinforcing bars were analyzed using Manson's hypothesis. The test results may seem to agree with the hypothesis.

Keywords : fatigue, deformed reinforcing bars, fracture mechanics, cold-work

1. INTRODUCTION

The problem of preventing fatigue failures in transportation structures is a primary concern of structural engineers. Extensive studies have been conducted to investigate the fatigue behavior of reinforcing bars. Most of these studies considered longitudinal reinforcing bars embedded in concrete beams because it was believed that this was the only suitable method to simulate the reinforcing bar forces experienced in actual concrete structures. Fatigue loading considerations for the United States have been reviewed in the American Concrete Institute (ACI) Committee 215 Reports[1),2)] and National Highway Cooperaive Research Program (NHCRP) Report 164[3)].

Since the development of current bar deformations and higher yield strength bars, studies have been performed to determine the fatigue behavior of reinforcing bars embedded in concrete beams. Few investigations of the fatigue characteristics for reinforcing bars alone have been conducted. Tests were conducted on reinforcing bars embedded in concrete to simulate the manner in which loads are transmitted to reinforcing bars. However, it is difficult to identify or isolate the effect of individual properties on the fatigue behavior of a reinforcing bar. Fatigue tests of reinforcing bars alone provide the investigator with more control over the specimen and allow some isolation of factors that influence the fatigue behavior. Several codes have provisions which limit the fluctuation stress of reinforcing bars in reinforced and prestressed concrete beams. However, there are no specifications or standards which address specifically the fatigue properties of the reinforcing bar. This may be because there are no standard methods for testing bars in fatigue, fatigue tests require special testing machines and relatively long periods of time, and fatigue properties of reinforcing bars may be influenced by several interrelated variables. Therefore,

* Member of JSCE, M. Eng., Assistant Chief Research Engineer, Track and Structure Laboratory Railway Technical Research Institute (2-8-38, Hikari-cho, Kokubunji-shi, Tokyo)

tests of reinforcing bars in air need to be performed to provide information that may aid in interpretation of beam fatigue tests, and possibly the development of more rational fatigue design provisions. In addition, a simple and reliable fatigue testing technique for reinforcing bars should be developed.

2. SCOPE OF INVESTIGATION

A series of axial-tension fatigue tests on small-diameter reinforcing bars was conducted to investigate the fatigue behavior of bars in air and the effects of cold-work on fatigue strength. They were analyzed using the fracture mechanics hyposesis.

3. TEST PROGRAM

This experimental investigation consists of two phases. In both studies, Grade 60 No. 3 (60 ksi (414 MPa) yield point stress and 3/8 in. (0.953 cm) diameter) straight reinforcing bars were used. In Phase I of the study, fatigue tests were conducted on 28 specimens to obtain the S-N curve for a normal reinforcing bars. Nine different magnitudes of constant-amplitude sinusoidal cyclic-load was used as the fatigue loading. The minimum stress was kept constant at 6 ksi (42 MPa) throughout the experiment.

In Phase II of the study, the fatigue tests were conducted on eight specimens to investigate the effect of pre-strain (cold-work) on fatigue life. Large strains, from 0.002 to 0.11 were induced statically in some of the test specimens by a hydraulic universal machine prior to fatigue loading.

(1) Test specimen

Grade 60, No. 3 deformed bars (Fig. 1) were used for the test specimens. The material properties are shown in Table 1. No thermal treatment nor surface treatment was applied. A typical stress-strain plot for a No. 3 deformed bar is shown in Fig. 2.

(2) Test assembly

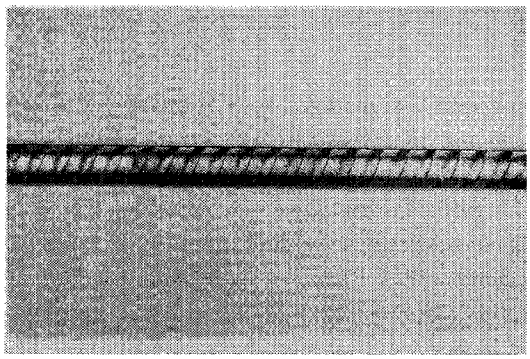

Fig. 1 Photograph of reinforcing bar (specimen).

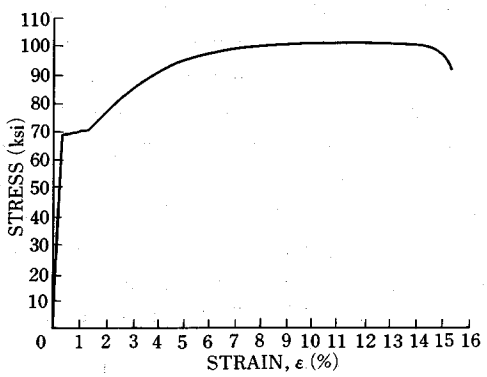

Fig. 2 Stress-strain curve of typical reinforcing bar.

In general, axial tension fatigue tests are not complicated tests. However, in order to test reinforcing bars in fatigue, several problems had to be overcome. The major problems were the method of gripping the specimen and the loading

Table 1 Material Properties for No. 3 Deformed Bars.

Items	Values
Grade Designation	ASTM A615 Grade 60 Deformed Billet-Steel Bar for Concrete Reinforcement
Heat Number	69803
Form of Product	No. 3 (3/8 in.) bar
Surface Condition	As-rolled
Lug Height	0.016 in. (0.04 cm)
Lug Spacing	0.24 in. (0.61 cm)
Tensile Strength	101 500 psi (700 MPa)
Yield Point	72 000 psi (496 MPa)
Elongation	15.3 % in 8 in. (20 cm) gage length
Modulus of Elasticity	29 500 000 psi (2.03×10^5 MPa)
Chemical Composition:	
C	0.42 %
Mn	1.07 %

system. No standard testing method to determine the fatigue properties of reinforcing bars has been developed in the United States. However, recommended procedures for axial tension fatigue tests of reinforcing bars in air may be found in the RILEM, FIP, and CEB Bulletin[4]. In this series of tests, this recommended test assembly was adopted. It was decided that an epoxy would be used to connect each test specimen to the anchorages. The length of the specimen was controlled by the loading machine available for conducting the tests. The length was approximately 4 ft 2 in (125 cm). Different types of test assemblies were used in the Phase I and Phase II studies. The details are shown in Fig. 3. The test assemblies were named Test Assembly A and Test Assembly B. Test Assembly A was used in the Phase I study and consisted of two anchorages for fatigue loading. Test Assembly B was used in the Phase II study and consisted of two anchorages for fatigue loading at the ends and two anchorages near the middle for static loading.

(3) Loading apparatus

The testing system, which was developed previously for a cable-stay fatigue study was used during this study. The testing system, shown in Figs. 4 and 5, consisted of a centerhole ram, extension chair, load cell, and split plates. The test assembly was passed through the center of the loading system. The loading system used was a closed-loop hydraulic servo-controlled system.

(4) Pre-straining

For the Phase II study, 0.2 to 11.3 percent strain was induced in some of the specimens prior to fatigue loading. Test Assembly B was used, and strain was induced with a 60-kip (27 t) hydraulic universal testing machine, gripping the anchorages (B) with the jaws of the testing machine. Strain was monitored over an 8 in. (20 cm) length between the B anchorages using an extensometer.

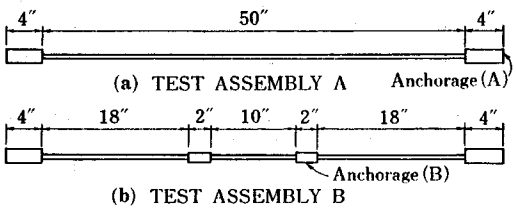

Fig. 3 Details of test assemblies.

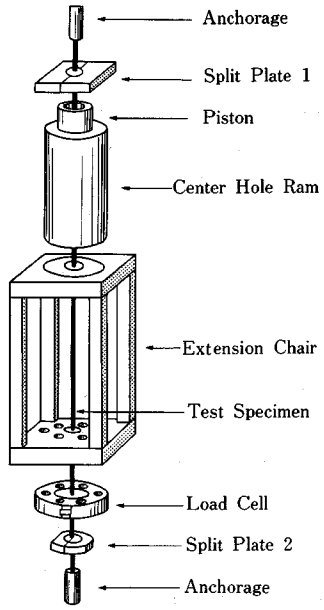

Fig. 4 Schematic of test setup.

4. TEST RESULTS

(1) Results of phase I study

A total of 28 reinforcing bars were tested using nine different stress ranges. Stresses were calculated using nominal areas of reinforcing bars (0.1104 in^2 (0.7123 cm^2)). The minimum stress was kept

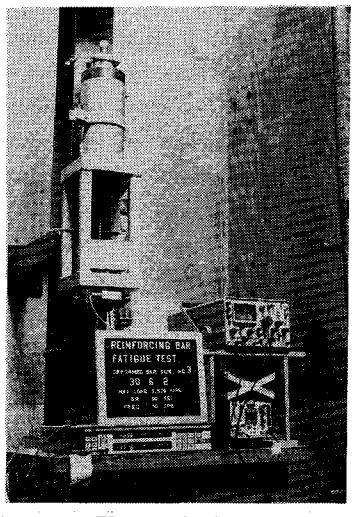

Fig. 5 Photograph of test setup.

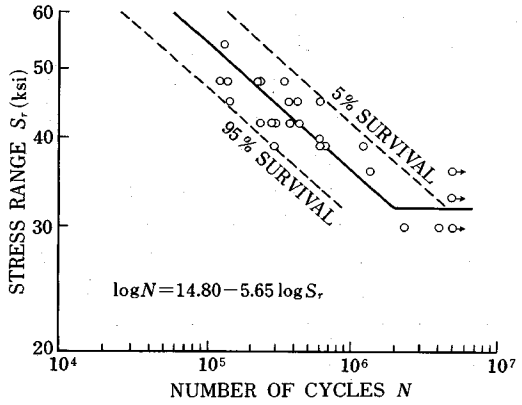

Fig. 6 S-N line for fatigue test data.

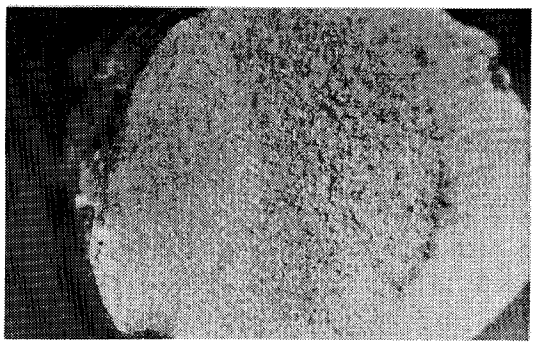

Fig. 7 Photograph of fractured section.

Table 2 Fatigue Test Results of Phase I Study.

Specimen Designation	Stress Range S_r (ksi)	Minimum Stress S_{min} (ksi)	Fatigue Life N	Frac. Section Position l^*	Location of crack Initiation
30-6-1	30.0	6.0	4 060 500	0.01	lug base
30-6-2	30.0	6.0	5 000 000+**	—	—
30-6-3	30.0	6.0	2 362 000	-0-	lug base
30-6-4	30.0	6.0	5 000 000+	—	—
33-6-1	33.0	6.0	5 000 000+	—	—
36-6-1	36.0	6.0	5 000 000+	—	—
36-6-2	36.0	6.0	1 369 530	0.26	lug base
39-6-1	39.0	6.0	675 890	0.39	lug base
39-6-2	39.0	6.0	613 980	0.26	lug base
39-6-3	39.0	6.0	1 225 400	0.12	lug base
39-6-4	39.0	6.0	659 000	0.15	lug base
39-6-5	39.0	6.0	296 250	-0-	lug base
40-6-1	40.0	6.0	607 990	0.25	lug base
42-6-1	42.0	6.0	238 120	0.11	lug base
42-6-2	42.0	6.0	298 340	0.20	lug base
42-6-3	42.0	6.0	376 500	-0-	lug base
42-6-4	42.0	6.0	439 120	0.16	lug base
42-6-5	42.0	6.0	284 970	0.26	lug base
45-6-1	45.0	6.0	609 280	0.01	lug base
45-6-2	45.0	6.0	142 090	0.01	lug base
45-6-3	45.0	6.0	423 550	0.42	lug base
45-6-4	45.0	6.0	369 330	-0-	lug base
48-6-1	48.0	6.0	224 880	0.09	lug base
48-6-2	48.0	6.0	344 520	-0-	lug base
48-6-3	48.0	6.0	226 080	-0-	lug base
48-6-4	48.0	6.0	121 810	-0-	lug base
48-6-5	48.0	6.0	138 000	-0-	lug base
54-6-1	54.0	6.0	131 600	0.20	lug base

* 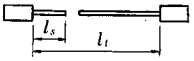

$l = l_s/l_t$

** Did not fail until 5 000 000 cycles.

constant at 6 ksi (42 MPa) for all tests, which was approximately 1/12 of the yield stress. The loading frequency was chosen as 600 cycles per minute (cpm) (=10 Hz). This high frequency was used because the fatigue life of specimens in air is not sensitive to loading frequencies up to 800 or 1 000 cpm. The sequence of numbers, 42-6-1 for example, represents the stress range (42 ksi (290 MPa)), minimum stress (6 ksi (42 MPa)), and specimen number in the sequence of tests for a given stress range. The stress range and fatigue life for each specimen are presented in Table 2 and Fig. 6. The ratio of failed section length between the fractured surface and the nearest anchorage to the total bar length between anchorages, and the location of the crack initiation are also presented in Table 2. Runouts are indicated by horizontal arrows in Fig. 6. Photographs of a fractured section is shown in Fig. 7.

(2) Results of phase II study

A total of eight specimens were tested to investigate the effect of pre-strain on fatigue life. The eight specimens were cut from two 20-ft (610 cm) lengths of reinforcing bar. The origin of each of the eight test specimens was recorded as Lot 1 or Lot 2. Six of the specimens were actually elongated (three from each lot) using a 60-kip (27 t) loading machine. Two of the specimens were not pre-strained to serve as control specimens. Test specimens were subjected to a stress range and minimum stress of 42 and 6 ksi (290 and 42 MPa), respectively. The loading frequency was 600 cpm (=10 Hz). The induced pre-strain (expressed as percent elongation), yield stress, maximum applied static stress, and fatigue life are presented in Table 3. The pre-strain history for each specimen is presented in Fig. 8. The ultimate strain for the

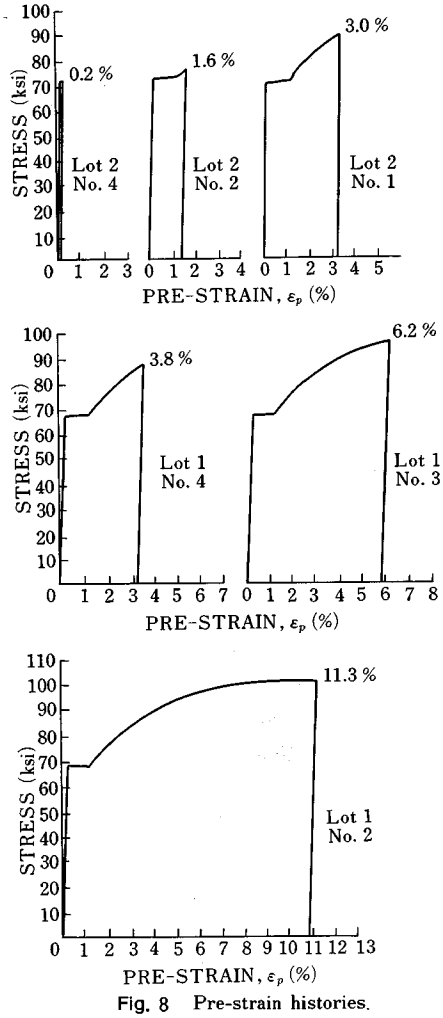

Fig. 8 Pre-strain histories.

Table 3 Fatigue Test Results of Phase II Study.

Lot	No.	Pre-Strain (% elongation)	Yield Stress S_y (ksi)	Maximum Stress S_{max} (ksi)	Fatigue Life N
1	1	0	—	—	194 400
	4	3.8	67.9	87.3	116 880
	3	6.2	67.9	96.0	78 830
	2	11.3	68.4	100.9	136 300
2	3	0	—	—	371 900
	4	0.2	72.5	72.5	367 650
	2	1.6	73.6	76.1	322 800
	1	3.0	70.7	88.9	199 360

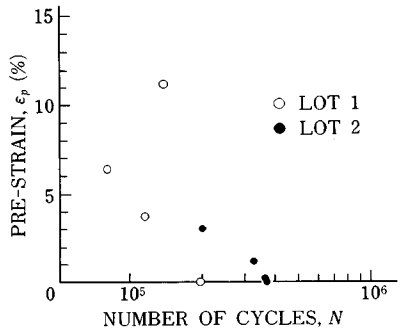

Fig. 9 Fatigue test results of Phase II study.

reinforcing bars was approximately 15.3 percent (see Fig. 2). A plot of pre-strain versus fatigue life is presented in Fig. 9. Even though the data are limited in number, trends appear to exist for both lots of data. However, the specimen with the largest pre-strain in Lot 1 exhibited a long fatigue life which did not agree with the trend demonstrated by the other test specimens in Lot 1.

5. EVALUATION OF TEST RESULT

(1) Fatigue strength of reinforcing bars

The evaluation of test data collected during this experimental investigation is carried out using a statistical approach and fracture mechanics techniques. The fatigue life of a reinforcing bar is primarily determined by the magnitude of stress range, and the most common graphical presentation of fatigue test data is the S-N diagram. This method is consistent with the recommended approach of ASTM E 468[5]. The determination of reasonable S-N diagrams or relationships for both finite-life and long-life regions is quite important. Various formulas to represent these relationships have been suggested since Wöhler pioneered studies in this area. In practical applications, linear or linearized S-N relationships are commonly used in the finite-life region. The equation of an S-N curve may be expressed as follows :

$$\log N = p + q \log S_r \quad \cdots\cdots (1)$$

Here, the fatigue life, N, is the dependent variable and the stress range, S_r (ksi), is the independent variable. As to evaluate the test results, the following regression line equation for the finite-life region and statistical values are obtained.

$$\log N = 14.8 - 5.65 \log S_r \quad \cdots\cdots (2)$$

Correlation coefficient, $R=-0.89$, Standard error of estimate, $S_e=-0.184$. Data and S-N curves for 5, 50 and 95 percent survival are shown in Fig. 6. The regression equation provides the 50 percent estimate of survival. The run-out data were excluded from the calculation of the regression line. The term "run-out" as used in this investigation describes test specimens which did not fail before five million cycles of load. The fatigue limit, which is empirically defined as the fatigue strength at a two million cycle fatigue life, was calculated as 32 ksi (221 MPa).

The major problems associated the analysis of fatigue test data and scatter of fatigue life, N, and run-out. The scatter in N is believed to be due primarily to the variation of properties of each specimen, differences in test conditions, and uncertainty in fracture process. In addition, the number of test data points collected during each investigation is relatively few, in general, because of time and cost concerns. Special considerations for statistical evaluation are necessary for fatigue test data. The popularly accepted theory of "order statistics" is being used to estimate the cumulative frequency distribution of test observations such as fatigue tests. This theory permits the estimation to be made from relatively small sample sizes.

The distribution of test data was evaluated on a probablility scale. The plotting positions, P_i, versus the logarithm of fatigue life, $\log N$, are presented in Table 4 and Fig. 10. The major interest is whether these points plot on a straight line. If these points are positioned on a straight line, the distribution of $\log N$ may be interpreted as a normal distribution. The average correlation coefficient for the four lines drawn through the 39, 42, 45 and 48 ksi (269, 290, 310 and 331 MPa) data, was 0.96 and for the line through the 30 ksi (207 MPa) data was 0.90. The low correlation coefficient value for the 30 ksi data resulted because run-out data was included this time. Through this evaluation, we may conclude that the finite-life of the test specimens follows a logarithmic-normal-distribution. As another statistical value, the slopes of these lines indicate the scatter of the test data. Steeper slopes indicate less scatter. The inverse slope, q', is presented in Table 4. For run-out data, it is possible to reconstruct the fatigue life to fit the points on the probability line if it is assumed that the distribution of fatigue life in the long-life region also follows the logarithmic-normal distribution and has the same variance as that of finite-life region. However, this has not been verified. Run-out test data was simply excluded in the calculation of the regression line.

(2) Effect of pre-strain (cold-work) on fatigue behavior of reinforcing bars

Previous studies of shear fatigue behavior of reinforced concrete beams[6] report that the primary location for the fracture of stirrups is at bent corners. In addition, fatigue strength of bent bars is approximately half of the fatigue strength of straight bars[6)~8)]. As one of the possible reasons for this

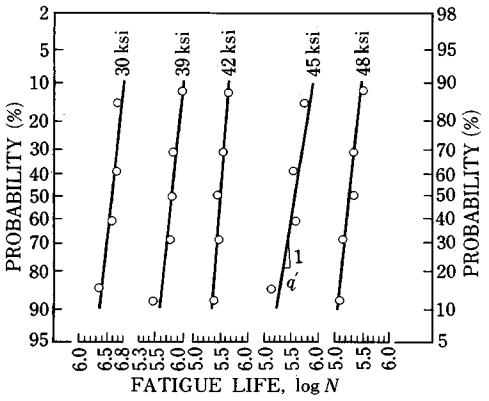

Fig. 10 Distribution of fatigue life data.

Table 4 Distribution of Fatigue Life Data.

		log N (S_r)				log N (S_r)	
i	P_i	39	42	48	i	P_i	30	45
1	11.9	5.47	5.38	5.09	1	14.7	6.37	5.15
2	31.0	5.79	5.45	5.14	2	38.2	6.60	5.57
3	50.0	5.82	5.47	5.35	3	61.8	6.70*	5.63
4	69.1	5.83	5.58	5.63	4	85.3	6.70*	5.78
5	88.1	6.09	5.64	5.54				
Inverse Slope q'		0.07	0.04	0.06	q'		0.05	0.08
Correlation Coefficient R		0.94	0.98	0.97	R		0.90	0.96

* N=5 000 000 run-out data

behavior, the effect of large tensile strains was studied. Manson's low cycle fatigue approach[9] was applied to analyze this behavior.

Stirrups and some longitudinal reinforcing bars are cold-worked or bent at construction sites or fabrication factories. As mentioned above, bending has been shown to reduce the fatigue strength of reinforcing bars. Some of the possible reasons for this behavior are :

① the effect of large tensile or compressive strains beyond yield strain,
② the change of configuration of surface deformations,
③ the effect of residual stress,
④ the effect of concentrated load transfer from concrete to the reinforcing bar at the bent location as the result of confining concrete.

These reasons have been qualitatively understood ; however, no investigations have been conducted to determine the contribution of these effects quantitatively. In this study, the most primitive reason, the effect of large tensile strain on fatigue life, was investigated.

In order to determine the amount of pre-strain, the minimum bend diameter measured on the inside of the bar in typical American codes, such as the ACI 318 code[10], AASHTO Specification[11] was used. The bend diameter for No. 3 reinforcing bars is defined as $4\,d_b$, where d_b is the diameter of bar, for stirrup applications. The fiber elongations or strain can be estimated assuming that the bar is a curved bar according to the equations in Ref. 12).

Taking r_1, r_2, and r_c as the inside surface radius, the outside surface radius, and the radius of the centroid, respectively :

$$r_1 = 4\,d_b \quad (3)$$

$$r_2 = r_1 + d_b = 5\,d_b \quad (4)$$

$$r_c = r_1 + d_b/2 = 4.5\,d_b \quad (5)$$

The distance between the centroid and the neutral axis, ε_c, is defined as follows :

$$\varepsilon_c = r_c - d_b/\log_e(r_2/r_1) = 1.858\times10^{-2}\,d_b \quad (6)$$

Assuming the bar is bent 90 degrees and no elongation is induced beyond the 90 degree arc, the arc lengths of the inside surface, outside surface, and neutral axis, l_1, l_2, and l_n, respectively, are expressed as follows :

$$l_1 = r_1\pi/2 \quad (7)$$

$$l_2 = r_2\pi/2 \quad (8)$$

$$l_n = (r_c - \varepsilon_c)\,\pi/2 \quad (9)$$

The fiber strains of the inside surface and outside surface, ε_1 and ε_2, respectively, are derived as follows :

$$\varepsilon_1 = (l_1 - l_n)/l_n = -0.107 \quad (10)$$

$$\varepsilon_2 = (l_2 - l_n)/l_n = 0.116 \quad (11)$$

Therefore, tensile strains, as large as 11 percent, may be induced in stirrups during their fabrication. Fig. 11 shows the effect of pre-strain as the ratio of the fatigue life of a pre-strained specimen to that of a non-pre-strained specimen, N/N_0, versus the amount of induced pre-strain. A trend in reduction of fatigue life with increase of pre-strain was observed except for the largest pre-strained specimen. However, the fatigue lives of all the pre-strained specimens fall within the 95 percent confidence interval obtained in Phase I study. In order to analyze this effect, low-cycle fatigue which is a field of study dealing with fatigue failures for large

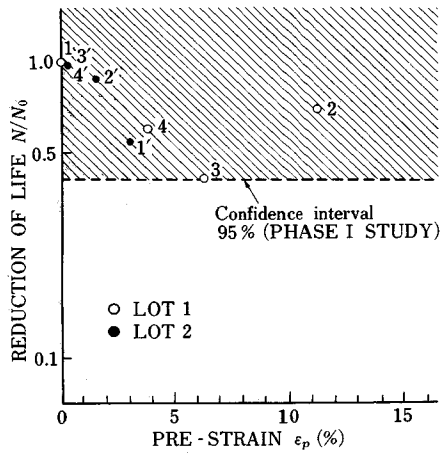

Fig. 11 Ratio of fatigue life of pre-strained specimen to that of non-pre-strained specimen versus amount of induced pre-strain.

amplitude strains was adopted.

Manson et al.[9] argued that the fatigue resistance of materials subjected to a given strain range could be estimated by superposition of the elastic and plastic strain components. The elastic component is described in terms of the stress range and number of loading cycles.

$$\Delta\varepsilon_e E = S_r = \alpha (N_f)^{\gamma} \quad (12)$$

where : $\Delta\varepsilon_e$=elastic strain range, E=modulus of elasticity, S_r=stress range, α=fatigue strength coefficient, N_f=number of cycles to failure, γ=fatigue crack growth rate exponent. The plastic component of strain is described by the Manson-Coffin[13] relationship.

$$\Delta\varepsilon_p = \beta (N_f)^{\delta} \quad (13)$$

where : $\Delta\varepsilon_p$=plastic strain range, β=fatigue ductility coefficient, N_f=number of cycles to failure, δ=fatigue ductility exponent.

Then, the total strain range, $\Delta\varepsilon_t$, is expressed as :

$$\Delta\varepsilon_t = \Delta\varepsilon_e + \Delta\varepsilon_p \quad (14)$$

Manson derived the total strain range equation, based on test results of 29 different types of structural steel, to be :

$$\Delta\varepsilon_t = 3.5 (S_u/E) N_f^{-0.12} + D^{0.6} N_f^{-0.6} \quad (15)$$

where : S_u=ultimate tensile strength (psi), D=ductility ; $\log_e (1/(1-r_a))$, r_a=reduction in area, E=modulus of elasticity (psi).

Manson also studied cumulative damage and found the superposition of elastic strain range and plastic strain range to follow the Minor cumulative damage law. This relationship can be expressed as :

$$\sum n_{pl}/N_{pl} + \sum n_{el}/N_{el} = 1 \quad (16)$$

where : n_{pl}=elapsed number of plastic strain cycles, n_{el}=elapsed number of elastic strain cycles, N_{pl}=number of cycles of failure by plastic strain, N_{el}=number of cycles to failure by elastic strain.

The pre-strain effect of fatigue life may be calculated using Eqs. (15) and (16). Because precise experimental data for ductility, D, in Eq. (15) is not available, the reduction in area to calculated the value of D was assumed to be proportional to the magnitude of the induced strain (pre-strain). The method to derive D from Eq. (15), is taking the total strain range, $\Delta\varepsilon_t$, as the ultimate strain, ε_{pu} (where ε_{pu}=0.153, see Table 1), and the number of cycles to failure, N_f, equal to one. The derivation of the value D is shown below. If the static loading test to ultimate is regarded as a one-cycle fatigue test, Eq. (14) can be expressed as :

$$\Delta\varepsilon_t = \Delta\varepsilon_p = \varepsilon_{pu} \quad (17)$$

where $\Delta\varepsilon_e$ is negligible. Then, substituting ε_{pu}=0.153, and N_f=1 into Eq. (15) :

$$0.153 = D^{0.6} 1^{-0.6} \quad (18)$$

The value of D is determined to be 0.044. The number of cycles to failure by plastic strain, N_{pl}, will be derived from Eq. (15), neglecting the elastic strain term. The plastic strain can be interpreted as the pre-strain.

$$\Delta\varepsilon_p = D^{0.6} N_{pl}^{-0.6}, \qquad N_{pl} = (\Delta\varepsilon_p/D^{0.6})^{-1/0.6} = D/(\Delta\varepsilon_p{}^{1/0.6}) \quad (19)$$

The process of pre-straining may be regarded as one cycle of fatigue loading and the elapsed number of plastic strain cycles, n_{pl}, is taken as one. Reduction of fatigue life, n_{el}/N_{el}, then becomes :

$$n_{el}/N_{el} = 1 - 1/N_{pl} = 1 - \Delta\varepsilon_p{}^{1/0.6}/D \quad (20)$$

The theoretical curve will be obtained substituting the value of D into Eq. (20). The reduction of fatigue strength, S_{rp}/S_{ro}, at N cycles will be given by Eq. (22) :

$$S_r = \Delta\varepsilon_e E = 3.5\, S_u N_f^{-0.12} \quad (21)$$

$$S_{rp}/S_{ro} = (N_{el}/n_{el})^{-0.12} \quad (22)$$

where : S_{rp}=fatigue strength at N cycles for the pre-strained specimen, S_{ro}=fatigue strength at N cycles for the non-pre-strained specimen.

On the other hand, the regression line equation shown in Eq. (2), which was obtained in Phase I

study, may be used instead of Eq. (21). Then, the relations of Eqs. (21) and (22) are re-written as follows.

$$S_r = 416\, N^{-1/5.65} \quad \cdots\cdots (23)$$

$$S_{rp}/S_{ro} = (N_{el}/n_{el})^{-0.177} \quad \cdots\cdots (24)$$

Comparison of these curves and the test results is shown in Fig. 12. Both these lines may seem to agree with the test results. However, the specimen with the largest pre-strain had a very long life. This increase in fatigue life may be the result of the radius of the lug base becoming larger due to significant elongation of the bar. The increase in the radius of the lug base may have resulted in a smaller stress concentration that initiated the fatigue cracks.

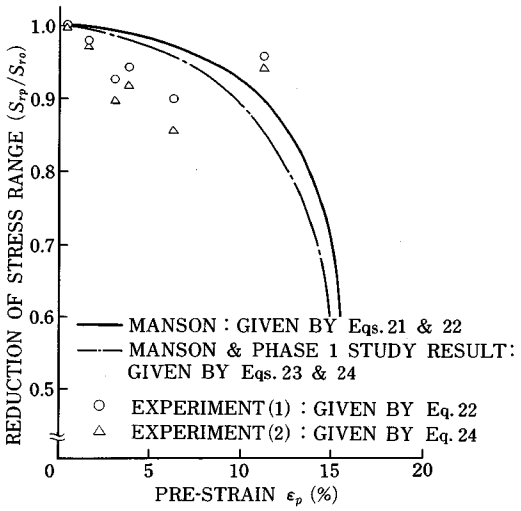

Fig. 12 Reduction of fatigue strength due to pre-strain as predicted using Manson solution.

From this result, the reduction of fatigue strength may be less than 15 percent in practical cases such as bent bars, because bend diameter for reinforcing bars are restricted by design codes and the induced fiber strain during fabrication may be calculated more or less 11 percent.

6. CONCLUSIONS

It is quite difficult to present general conclusions from the limited number of fatigue test results. However, the knowledge obtained through this investigation is summarized below.

(1) The mean fatigue life of Grade 60 No. 3 reinforcing bars was predicted by the following relation : $\log N = 14.8 - 5.65 \log S_r$, where N is the fatigue life in number of cycles and S_r is the stress range in ksi. This relation and the body of test data indicate that the fatigue limit is 32 ksi (221 MPa), which corresponds with a two million cycle fatigue life.

(2) The effect of pre-strain on the fatigue life of reinforcing bars may be explained by the low-cycle fatigue approach for pre-strains and the effect of large tensile strains beyond yield strain on reduction of fatigue strength may be less than 15 percent in practical cases.

7. ACKNOWLEDGEMENTS

The author gratefully acknowledges and thanks Professor Michael E. Kreger, Karl H. Frank, and John E. Breen for their supervision and friendship during this investigation. This research was conducted at the Phil M. Ferguson Structural Engineering Laboratory at the Balcones Research Center at The University of Texas at Austin in 1984.

REFERENCES

1) Nordby, G. M. : Fatigue of Concrete—A Review of Research, Journal of the Americal Concrete Institute, Proceedings Vol. 55, No. 2, pp. 191~220, August 1958.

2) ACI Committee 215 : Considerations for Design of Concrete Structures Subjected to Fatigue Loading, Journal of the American Concrete Institute, Vol. 73, No. 3, pp. 97 ~121, March 1974.

3) Helgason, T., Hanson, J. M., Somes, H. F., Corley, W. G. and Hognestad, E. : Fatigue Strength of High-Yield Reinforcing Bars, Report 164, National Cooperative Highway Research Program, Washington (1976).

4) CEB Application Manual on Concrete Reinforcement Technology, Bulletin d'information No. 140, Comité Euro-International du Béton (Paris), December 1981.

5) ASTM E 468 : Standard Recommended Practice for Presentation of Constant Amplitude Fatigue Test Results for Metallic Materials, Annual Book of ASTM Standards, American Society for Testing and Materials (Philadelphia).

6) Okamura, H., Farghaly, S. A. and Ueda, T. : Behavior of Reinforced Concrete Beams with Stirrups Failing in Shear under Fatigue Loading, Journal of Japan Society for Civil Engineers, Proceedings, No. 308, pp. 109 ~122, April 1981.
7) Rehm, G. : Contributions to the Problem of the Fatigue Strength of Steel bars for Concrete Reinforcement, Preliminary Publication, 6 th Congress of the IABSE (Stockholm, 1960), International Association for Bridge and Structures Engineering, Zurich, pp. 35~46, 1960.
8) Pfister, J. F. and Hognestad, E. : High Strength Bars as Concrete Reinforcement, Part 6, Fatigue Tests, Journal of the PCA Research and Development Laboratories, Vol. 6, No. 1, pp. 65~84, January 1964.
9) Manson, S. S. : Fatigue ; A Complex Subject—Some Simple Approximations, Experimental Mechanics, Vol. 5, No. 7, pp. 193~226, July 1965.
10) ACI 318-83, Building Code Requirements for Reinforced Concrete, American Concrete Institute (Detroit).
11) AASHTO, Standard Specifications for Highway Bridges, American Association of State Highway and Transportation Officials (Washington).
12) Timoshenko, S. : Strength of Materials Part 1, Robert E. Krieger Publishing Co. (New York).
13) Coffin, L. F. : A Study of the Effects of Cyclic Thermal Stresses on a Ductile Metal, Transactions of the American Society of Mechanical Engineers, Vol. 76, pp. 931, August 1954.

(Received November 27 1987)

圧密解析ソフトパソコンに上陸!!

地盤の非定常圧密解析プログラム

Mr.圧密

(特長)

- 非定常FEMによる線形弾性解析(christian系の解法)。
- 二次元平面歪解析。
- 要素として三角形・任意四角形が扱える。
- スケーリングをしているので安定して解が求まる。
- リスタート機能の完備。
- 入力はわかりやすいコマンド形式を採用(フリーフォーマット)。
- 図化処理(プロッタ、画像出力)等、豊富な機能を持つポストプログラムを完備。
- ジェネレート機能(長方形要素)により簡単にモデル作成が可能。
- 大モデルはそのままCRCネットワークでも(ホスト処理)可能。

販売価格：60万円　機種：NEC PC9800シリーズ 他

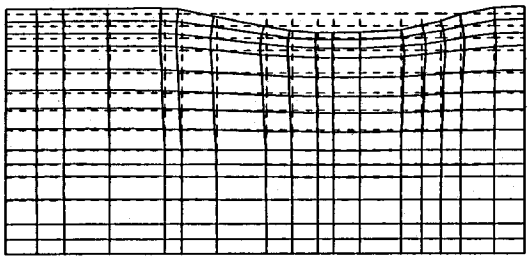

変 形 図

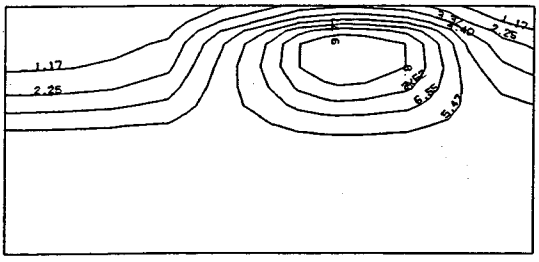

過剰間隙水圧コンター図

※EWS、汎用機用の圧密解析プログラム(逆解析も可能)として"UNICON"も用意しております。

CRC センチュリリサーチセンタ株式会社
大阪市東区北久太郎町4－68
(06－241－4121)担当:浜口・榊原

昭和三十七年五月二十六日 第三種郵便物認可
昭和六十三年八月十五日 印刷（毎月一回）
昭和六十三年八月二十日 発行（二十日発行）
土木学会論文集

土木学会論文集

定価一五〇〇円